한국소성가공학회 2005년도 춘계학술대회 논문집 pp. 155~158

석출 강화된 단결정의 소성변형에 관한 모델링

김준형 [1]· 한정석 [2]· 정관수#· 강태진 [1]

Modeling the Plastic Deformation of Crystals with Thin Precipitates

J. H. Kim, C. S. Han, K. Chung, T. J. Kang

Abstract

Precipitates, present in most commercial alloys, can have a strong influence on strength and hardening behavior of a single crystal. The effect of thin precipitates on the anisotropy of initial slip resistance and hardening behavior of crystals is modeled in this article. For the convenience of the computational derivation and implementation, the material formulation is given in the unrotated intermediate configuration mapped by the plastic part of the deformation gradient. Material descriptions for the considered two phased aggregates consisting in lattice hardening as well as isotropic hardening and kinematic hardening are suggested. Numerical simulations of various loading cases are presented to discuss and assess the performance of the suggested model.

Key Words : Crystal plasticity; Particulate reinforced materials; Hardening; Finite Elements

1. Introduction

Precipitation strengthening is one of classical approaches to enhance the initial strength and hardening behavior of metals. The influences of precipitates on the mechanical characteristics of crystals and in metallic alloys have been investigated by various authors [1-4]. From these investigations, it is known that the size, shape, spacing and orientation of precipitates, which can be altered during aging processes, have strong influence on the plastic behavior. While precipitates can influence the initial yield strength and its anisotropy, they can also dominate the hardening behavior, in particular, control kinematic hardening effects. With the influence precipitates have on single crystals, corresponding effects on the anisotropy of widely applied polycrystalline materials with precipitates can be expected. In this context, it is desirable to establish an elaborate model which can represent the effect of precipitates on the plastic anisotropy of initial yield strength as well as the isotropic hardening and kinematic hardening on single crystals. In this paper, the effect of thin precipitates on the anisotropy of the initial slip resistance, the isotropic hardening and the kinematic hardening is modeled and numerical simulations are performed.

2. Notations and constitutive setting

Kinematic relations, stress/strain-expressions and governing relations in the intermediate configuration $\tilde{B}$ in the conventional crystal plasticity are summarized in

1. 서울대학교 재료공학부
2. Max-Planck-Institut fuer Eisenforschung
교신저자: 서울대학교 재료공학부
E-mail: kchung@snu.ac.kr

the Table 1. Therein, the decomposition (1) of deformation gradient $\mathbf{F}$ into elastic $\mathbf{F}_e$ and plastic part $\mathbf{F}_p$ is applied, where it is assumed that the rotation of the lattice is contained in $\mathbf{F}_e$ (see Fig. 1). The plastic velocity gradient can be expressed with (4), where $\dot{\gamma}^\alpha$ denotes the plastic shearing rate, $\tilde{\mathbf{s}}^\alpha$ the slip direction and $\tilde{\mathbf{m}}^\alpha$ the slip plane normal of slip system α in $\tilde{B}$ with $|\tilde{s}^\alpha| = |\tilde{m}^\alpha| = 1$ and $\tilde{\mathbf{s}}^\alpha \cdot \tilde{\mathbf{m}}^\alpha = 0$.

Table 1 Kinematic relations, stress/strain expressions and governing relations in the intermediate configuration $\tilde{B}$ in crystal plasticity.

Multiplicative decomposition	$\mathbf{F} = \mathbf{F}_e \mathbf{F}_p$	(1)
velocity gradient	$\mathbf{l} = \mathbf{l}_e + \mathbf{F}_e \tilde{\mathbf{L}}_p \mathbf{F}_e^{-1}$	(2)
	with $\mathbf{l}_e = \dot{\mathbf{F}}_e \mathbf{F}_e^{-1}$	
	and $\tilde{\mathbf{L}}_p = \dot{\mathbf{F}}_p \mathbf{F}_p^{-1}$	(3)
Plastic velocity gradient	$\tilde{\mathbf{L}}_p = \sum_\alpha \dot{\gamma}^\alpha (\tilde{\mathbf{s}}^\alpha \otimes \tilde{\mathbf{m}}^\alpha) = \tilde{\mathbf{D}}_p + \tilde{\mathbf{W}}_p$	(4)
	$\tilde{\mathbf{D}}_p = \sum_\alpha \dot{\gamma}^\alpha (\tilde{\mathbf{s}}^\alpha \otimes \tilde{\mathbf{m}}^\alpha)_s$	(5)
	$\tilde{\mathbf{W}}_p = \sum_\alpha \dot{\gamma}^\alpha (\tilde{\mathbf{s}}^\alpha \otimes \tilde{\mathbf{m}}^\alpha)_a$	(6)
Lagrangian strain tensor	$\tilde{\mathbf{E}} = \frac{1}{2}(\mathbf{F}_e^T \mathbf{F}_e - \mathbf{F}_p^{-T} \mathbf{F}_p^{-1}) = \tilde{\mathbf{E}}_e + \tilde{\mathbf{E}}_p$	(7)
	$\tilde{\mathbf{E}}_e = \frac{1}{2}(\mathbf{F}_e^T \mathbf{F}_e - \mathbf{1})$	(8)
	$\tilde{\mathbf{E}}_p = \frac{1}{2}(\mathbf{1} - \mathbf{F}_p^{-T} \mathbf{F}_p^{-1})$	(9)
Second Piola-Kirchhoff stress	$\tilde{\mathbf{S}} = \mathbf{F}_e^{-1} \boldsymbol{\tau} \mathbf{F}_e^{-T}$	(10)
Mandel stress	$\tilde{\mathbf{P}} = (\mathbf{1} + 2\tilde{\mathbf{E}}_e)\tilde{\mathbf{S}} = \tilde{\mathbf{C}}_e \tilde{\mathbf{S}}$	(11)
Isotropic relation	$\tilde{\mathbf{S}} = \tilde{\mathbf{\Gamma}}_e \tilde{\mathbf{E}}_e$	(12)
Resolved shear stress	$\tau^\alpha = \tilde{\mathbf{P}} \cdot (\tilde{\mathbf{s}}^\alpha \otimes \tilde{\mathbf{m}}^\alpha)_s$	(13)
Yield function	$\Phi^\alpha = \lvert\tau^\alpha - x^\alpha\rvert - g^\alpha$	(14)
Kuhn-Tucker-type conditions	$\mathrm{sgn}(\tau^\alpha - x^\alpha)\dot{\gamma}^\alpha \geq 0 \quad \Phi^\alpha \leq 0$ $\dot{\gamma}^\alpha \Phi^\alpha = 0$	(15)

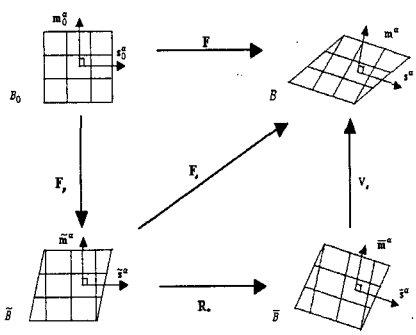

Fig. 1 Intermediate configurations obtained by $\mathbf{F} = \mathbf{F}_e \mathbf{F}_p = \mathbf{V}_e \mathbf{R}_e \mathbf{F}_p$.

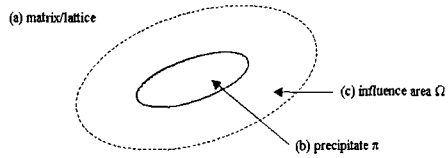

Fig. 2 Influence area Ω around a precipitate π.

3. Evolution equations for the hardening

In view of Fig. 2, the resolved shear stress is divided into three parts: the average resolved shear stress of the lattice τ_M^α, the average stress in the influence region τ_Ω^α weighted with the relevant area fraction ω and the average of the stress within the inclusion τ_I^α weighted with the relevant volume fraction f, yielding

$$\tau^\alpha = (1 - f - \omega)\tau_M^\alpha + \omega \tau_\Omega^\alpha + f \tau_I^\alpha . \tag{16}$$

For incorporation of such a model with the internal variable approach, the different stress components weighted with their area and volume fractions are

$$\hat{\tau}_\Omega^\alpha = \omega(\tau_\Omega^\alpha - \tau_M^\alpha) \quad \text{and} \quad \hat{\tau}_I^\alpha = f(\tau_I^\alpha - \tau_M^\alpha) \tag{17}$$

yielding

$$\tau^\alpha = \tau_M^\alpha + \hat{\tau}_\Omega^\alpha + \hat{\tau}_I^\alpha . \tag{18}$$

The influence area ω may be dependent on the size of the precipitate. For simplicity, however, it is assumed that ω is proportional to f, which yields both hardening components $\hat{\tau}_\Omega^\alpha$ and $\hat{\tau}_I^\alpha$ to be proportional to f in (17).

As correspondence to the internal variables applied in·

(14), it is suggested to correlate the slip resistance to the hardening mechanisms of the matrix $g^\alpha = \tau_M^\alpha + \hat{\tau}_\Omega^\alpha$ and, following Bate et al. [2], the back stress to the stress in the precipitate, as $x^\alpha = \hat{\tau}_I^\alpha$. In average, the elastic range and thus also the back stresses are assumed to be smaller in other regions than in the precipitate. The kinematic hardening related to Ω is, therefore, as for other regions of the lattice, neglected.

Thin precipitates, considered here, like the θ' precipitates, are normally aligned parallel to the habit planes (see Fig. 3) after the aging process. The volume fraction of each habit plane can vary depending on the aging process. In the deformation process of the aggregate, the inhomogeneous deformation is in part accommodated by rotations precipitates relative to the lattice (see Fig. 4).

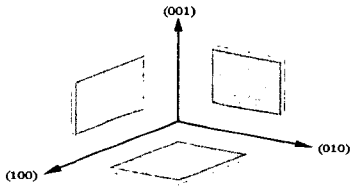

Fig. 3: Precipitates in habit planes.

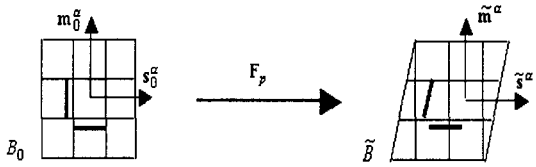

Fig. 4 Rotation of precipitates by $\mathbf{F}_p$.

All hardening descriptions of the suggested material model are summarized in Table 2. In Table 2, the fourth order tensor $\tilde{\mathbf{H}}^\pi$ is defined as

$$\tilde{\mathbf{H}}^\pi = \sum_{ijkl}^{3} H_{ijkl}^\pi \tilde{\mathbf{e}}_i^\pi \otimes \tilde{\mathbf{e}}_j^\pi \otimes \tilde{\mathbf{e}}_k^\pi \otimes \tilde{\mathbf{e}}_l^\pi \tag{19}$$

with the base vectors of the precipitates $\tilde{\mathbf{e}}_i^\pi$. The components of $\tilde{\mathbf{H}}^\pi$ can be given with $H_{ijkl}^\pi = 1$ for $i = j = k = l$, $(i, j, k, l) = (2, 3, 2, 3)$, $(i, j, k, l) = (3, 2, 3, 2)$ and otherwise $H_{ijkl}^\pi = 0$ for a platelet precipitate aligned to [100] plane and $\tilde{\mathbf{e}}_i^\pi$ parallel to (100), (010), and (001), respectively. The expressions for $\tilde{\mathbf{H}}^\pi$ aligned to other habit planes are then obtained by rotation of $\tilde{\mathbf{e}}_i^\pi$, $i = 1, 2, 3$.

Table 2 Hardening descriptions for a single crystal with thin precipitates

Slip resistance

$$\dot{g}^\alpha = \sum_\beta \left(h_M^{\alpha\beta} + h_\Omega^{\alpha\beta}\right)\left|\dot{\gamma}^\beta\right| \tag{20}$$

Work hardening moduli of the lattice

$$h_M^{\alpha\beta} = [q_M + (1 - q_M)\delta^{\alpha\beta}]h_M^\beta \tag{21}$$

$$h_M^\beta = \tau_M^0 \left(\frac{c_M \gamma}{b_M \tau_M^0} + 1\right)^{b_M} \tag{22}$$

Moduli related to the hardening induced by precipitates

$$h_\Omega^{\alpha\beta} = [q_M + (1 - q_M)\delta^{\alpha\beta}]h_\Omega^\beta \tag{23}$$

$$h_\Omega^\alpha = \frac{1}{f}\sum_\pi f^\pi h_\Omega^{\pi\alpha} \sqrt{(\tilde{\mathbf{s}}^\alpha \otimes \tilde{\mathbf{m}}^\alpha)_S \cdot \tilde{\mathbf{H}}^\pi (\tilde{\mathbf{s}}^\alpha \otimes \tilde{\mathbf{m}}^\alpha)_S} \tag{24}$$

$$h_\Omega^{\pi\alpha} = h_\Omega^o \sec h^2 \left(\frac{h_\Omega^o \gamma}{\tau_\Omega^s - \tau_\Omega^o}\right) \tag{25}$$

Kinematic hardening induced by precipitates

$$\hat{\tau}_I^\alpha = x^\alpha = \tilde{\mathbf{C}}_e \tilde{\mathbf{X}} \cdot (\tilde{\mathbf{s}}^\alpha \otimes \tilde{\mathbf{m}}^\alpha)_S \tag{26}$$

$$\tilde{\mathbf{X}}^\nabla = c_x f \tilde{\mathbf{\Gamma}}_e \tilde{\mathbf{H}} \sum_\beta \dot{\gamma}^\beta (\tilde{\mathbf{s}}^\beta \otimes \tilde{\mathbf{m}}^\beta)_S - b_x \left|\dot{\gamma}\right| \tilde{\mathbf{X}} \tag{27}$$

$$\tilde{\mathbf{H}} = \frac{1}{f}\sum_\pi f^\pi \tilde{\mathbf{H}}^\pi \tag{28}$$

4. Numerical examples

The numerical algorithm has been implemented into the ABAQUS explicit (2002) material user interface and all simulations have been performed explicitly. The step sizes have been chosen in such a way that the kinetic energy is negligible compared to the strain energy.

To illustrate the plastic anisotropy in the initial yield of the suggested model, tensile deformation of Al-xCu crystals with different microstructures are considered. To illustrate the performance of the proposed approach, numerical calculations have been preformed and results in the initial yield stress were compared with

experimental results obtained by Zhu et al. [4] and predictions listed therein obtained by the models suggested in Hosford & Zeisloft [1] and Bate et al. [2]. As shown in Table 3, our proposed model yields closer results to those obtained experimentally than the models of Hosford & Zeisloft [1] and Bate et al. [2].

Table 3 Comparison between experimental and simulation results for the modified axial component of the initial yield stress, τ_{axial} in the stress-free-aged and stress-aged Al-Cu specimens.

Specimen number	Experimental results*		Simulation results		
	τ_{axial}^{ex} (Mpa)	δ^{ex} (%)	δ	δ^{H} **	δ^{B} ***
1f	80	-15.3	-7.9	-6.1	-33.6
1s	67.8				
2f	78	-13.1	-7.7	-17.1	-26.5
2s	67.8				
3f	79.2	-12.4	-7.7	-7.9	-31.9
3s	69.4				
4f	68.6	-12.0	-7.5	2.1	-41.8
4s	60.4				
5f	67.8	-22.3	-7.4	-3.4	-36.4
5s	52.7				
6f	63.7	-3.9	-3.6	1.2	21.9
6s	61.2				

* Data from Zhu et al. [4]
** δ^{H} : predicted by Hosford's plastic inclusion model
*** δ^{B} : predicted by Bate's elastic inclusion model

5. Conclusions

The effect of the thin precipitates on the anisotropy of the initial slip resistance and isotropic-kinematic hardening has been modeled in this article. From the results of the numerical simulation it is found that the suggested model represents the initial plastic anisotropy at least qualitatively well and that it has an improved representation of various characteristic hardening behaviors in comparison with conventional hardening descriptions where the precipitate structure is not reflected.

Acknowledgement

This work was supported by the Ministry of Science and Technology through the National Research Laboratory of Korea.

References

[1] W. F. Hosford, R. H. Zeisloft, 1972, The anisotropy of age-hardened Al-4 Pct Cu single crystals during plane-strain compression, Metall. Trans., Vol. 3, pp. 113-121.

[2] P. Bate, W. T. Roberts, D. V. Wilson, 1981, The plastic anisotropy of two-phase aluminum alloys-I. Anisotropy in unidirectional deformation, Acta Metal., Vol. 29, pp. 1797-1814.

[3] F. Barlat, J. Liu, 1998, Precipitate-induced anisotropy in binary Al-Cu alloys, Mat. Sci. Eng., A 257, pp. 47-61.

[4] A. W. Zhu, J. Chen, E. A. Starke Jr., 2000, Precipitation strengthening of stress-aged Al-xCu alloys, Acta. Mat., Vol. 48, pp. 2239-2246.